Elastic diffuse scattering of neutrons in FeNi Invar alloys

Y. Tsunoda,[1] L. Hao,[1] S. Shimomura,[2] F. Ye,[3] J. L. Robertson,[3] and J. Fernandez-Baca[3]

[1]*School of Science and Engineering, Waseda University, 3-4-1, Ohkubo, Shinjuku, Tokyo 169-8555 Japan*
[2]*Faculty of Science and Technology, Keio University, 3-14-1, Hiyoshi, Kohoku-ku, Yokohama, Kanagawa 223-8522, Japan*
[3]*Oak Ridge National Laboratory, Oak Ridge, Tennessee 37831-6393 USA*

Elastic diffuse scattering of neutrons was found around various Bragg-peak positions in FeNi Invar alloys. The diffuse scattering intensities depend on the temperature and Ni concentration. The intensities increase with decreasing temperature and decrease with increasing Ni concentration. The distribution of diffuse scattering intensity changes from peak to peak and is well explained by the formation of clusters with a lattice deformation consisting of a shear wave propagating along the $\langle 1\ 1\ 0 \rangle$ direction and with the $\langle 1\ -1\ 0 \rangle$ polarization vector. The ranges of temperature and Ni concentration, for which diffuse scattering is observed, coincide with those for which the Invar anomalies are observable. The origin of the clusters together with the lattice deformation and their role with regard to the Invar effects are discussed as well as the possibility of a precursor for the fcc-bcc martensitic transformation observed in FeNi alloys.

I. INTRODUCTION

The Invar effect of FeNi alloys was found by Guillaume[1] more than 100 years ago. Since the FeNi Invar alloy at a Ni concentration around 35 at. % shows an almost zero value of thermal-expansion coefficient over a wide temperature range around room temperature, it has long been applied to the products of high-precision mechanical instruments. Due to this industrial importance, many experimental and theoretical works have been carried out on FeNi Invar alloys in an effort to better understand their properties. In spite of these efforts, the microscopic origin of the Invar effect has not yet well understood. Nowadays, the most accepted explanation is the Weiss's 2γ-state model. Since various anomalous properties of the Invar alloys seem to be related to the magnetism of Fe in an fcc structure, Weiss[2] proposed that there are two possible energetically degenerate states for fcc Fe, a high-spin state with large atomic volume and a low-spin state with small atomic volume. At low temperature, the majority of fcc Fe occupies the high-spin state. With increasing temperature, Fe atoms are excited to the low-spin state. The loss of atomic volume in this process compensates the normal thermal expansion caused by the unharmonicity of the lattice potentials, resulting in a zero thermal-expansion coefficient. Various properties of Invar alloys reported before 1990 were summarized by Wasserman.[3] Since the 2γ-state model is related to the magnetic ground state of fcc Fe, it stimulated many theoretical works. Modern first-principles calculations seem to be consistent with this 2γ-state model except for minor inconsistencies with experiments.[4–8] These theories derived two magnetic states with different sizes of magnetic moments and atomic volumes with almost the same energies for fcc FeNi alloys. However, the theoretically derived transition between these two states is always of the first order,[6,7] while there is no indication of the first-order transition experimentally for the FeNi alloys in the fcc phase. To overcome these difficulties, new calculations were recently performed.[9,10] Introducing the noncollinear spin configuration in the low-volume state, authors succeeded in explaining the continuous

transition from the ferromagnetic high-spin state to the noncollinear low-spin state with small atomic volume. To verify the existence of the noncollinear spin component in FeNi Invar alloys, neutron polarization analysis measurements were performed using powder sample.[11] Results were rather negative. All transverse spin components observed in this measurement were ascribed to be magnon excitations. Furthermore, the theoretically derived 2γ-state model itself was examined using polarized neutrons.[12] In the theory, the ratio of electronic configurations of the $3d$ electrons with e_g and t_{2g} symmetries should change through the transition between these two states.[5] Results were again negative. Thus, in the present stage, the 2γ-state model is still not definitive on the experimental side although many theoretical calculations support this model.

The present experiments started trying to observe the noncollinear spin components of Fe spins in the Invar alloy[13] using single-crystal samples. We found elastic diffuse scattering located around the various Bragg-peak positions. The scattering intensities strongly depended on temperature. However, from various properties of the diffuse scattering, it is considered that the diffuse scattering is not magnetic in origin but comes from a local lattice deformation. Experimental data and analysis are given in Secs. III and IV, respectively. The observed intensity contour maps are well reproduced by a simple model with a Gaussian distribution of diffuse peaks and explained by the presence of clusters with a lattice deformation arising from a shear wave propagating along the $\langle 1\ 1\ 0 \rangle$ direction. The intensity variation of the diffuse scattering seems to have strong correlations with the Invar effect. In Sec. V, we discuss the influence of clusters along with the lattice deformation associated with the Invar effect and the possibility of the formation of premartensitic embryos of an fcc-bcc martensitic transformation in FeNi alloys. Section VI is devoted to the conclusions of the present experiments.

II. SAMPLE PREPARATION AND EXPERIMENTS

Several single crystals of $Fe_{1-x}Ni_x$ alloys ($x=0.35$, 0.40, 0.50, and 0.60) including pure Ni were grown in an Al_2O_3

crucible using a furnace with a carbon electrode. Each crystal has a volume of about 1.5 cc. All of the alloy crystals were used in the as-grown state. Since the speed of decreasing temperature around 1200 K for this furnace is rather fast (120 K/min), the development of atomic short-range order (ASRO) would be suppressed considerably.

Preliminary neutron-scattering measurements were performed at the T1-1 triple-axis spectrometer installed on the thermal guide of JRR-3M (Tokai) using a pyrolytic graphite (PG) monochromator and PG analyzer. Since the incident neutron energy was fixed at 14.4 meV for this spectrometer, the diffuse peaks around the 1 1 1 and 2 0 0 Bragg-peak positions were accessible. Temperature and concentration dependences for diffuse peaks around these Bragg-peak positions were mainly studied. In order to remove higher order contamination, a thick PG filter was used. Collimators of 40′, 40′, and 40′ were used between monochromator and sample, the sample and analyzer, and the analyzer and detector, respectively.

Measurements on additional Bragg-peak positions were performed at the HB-3 triple-axis spectrometer at HFIR, Oak Ridge National Laboratory using a Si (1 1 1) monochromator together with a PG analyzer. Most of the data were taken using an incident neutron energy of 30.5 meV. For the data around the 2 2 2 Bragg-peak position, an incident neutron energy of 35 meV was used. A high-temperature displex was used for taking both low- and high-temperature data.

All data for both T1-1 and HB-3 were taken using a PG analyzer set to the elastic condition in order to avoid inelastic-scattering contamination. The energy resolutions for elastic incoherent peaks were 0.66 meV for T1-1 and 1.2 meV for HB-3 in full width at half maximum (FWHM), respectively.

III. EXPERIMENTAL DATA

We first found a typical butterfly pattern of diffuse scattering around the 2 0 0 Bragg-peak position for the $Fe_{65}Ni_{35}$ alloy at the T1-1 triple-axis spectrometer. To elucidate the cause of diffuse scattering, the temperature dependence of diffuse scattering was studied. In Fig. 1, diffuse scattering intensity contour maps around 2 0 0 obtained at 32, 300, and 600 K are given together with the difference between 32 and 300 K. In these figures, the ridge extending along the [0 1 0] direction (the body of the butterfly) comes from the mosaic spread of the single crystal. The diffuse scattering intensity shows the maximum value at the lowest temperature and decreases as the temperature increases. At 600 K, the butterfly pattern completely disappears and changes into a circular pattern. The latter should be ascribed to magnetic critical scattering because the Curie temperature is rather close to 600 K ($T_c \sim 550$ K). Note the drastic change in the intensity between 32 and 300 K.

Another important factor needed to investigate the cause of diffuse scattering is the composition dependence of the alloys. An example of the data for different Ni compositions is given in Fig. 2. These data were taken around the 2 0 0 Bragg-peak position in the (0 0 1) scattering plane at room temperature under the same experimental conditions. The
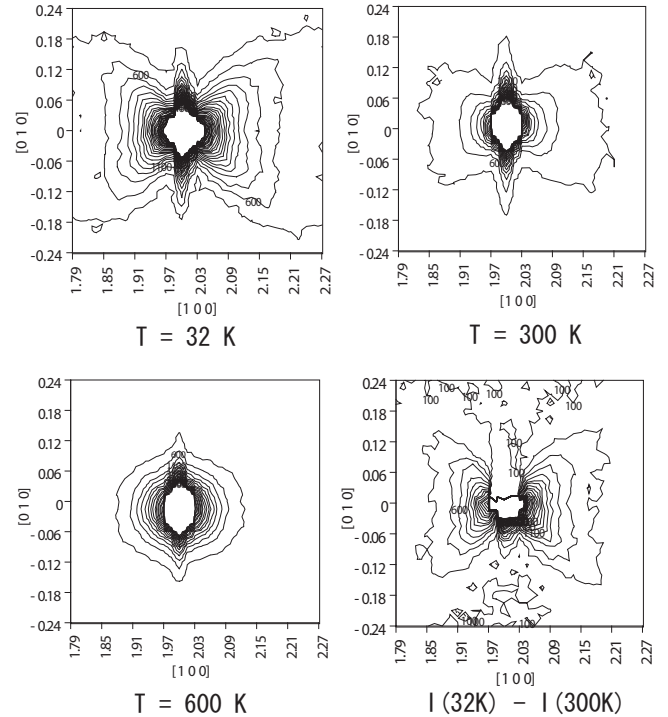

FIG. 1. Temperature variation of elastic diffuse scattering intensity contour maps around the 2 0 0 Bragg-peak position for $Fe_{65}Ni_{35}$ alloy studied by the T1-1 triple-axis spectrometer at Tokai. Subtracted data are also given. Numbers in the maps indicate the scattering intensities.

diffuse scattering intensity decreases with increasing Ni composition. We have also studied the diffuse peaks around the 0 0 2 Bragg-peak positions in the (1 −1 0) scattering plane for alloys with different Ni concentrations, and consistent results were obtained. For pure Ni, no diffuse peak was observed except for the small contour observed close to the Bragg-peak position. This would be ascribed to be a contamination of phonons observed within the energy resolution.

Diffuse scattering around various Bragg-peak positions was examined for an $Fe_{65}Ni_{35}$ alloy at the HB-3 triple-axis spectrometer using a Si (1 1 1) monochromator. The intensity contour maps obtained at low temperature (~ 10 K) are given in Fig. 3 for various Bragg-peak positions. Some data were contaminated by Al powder lines used for the support of the $Fe_{65}Ni_{35}$ single crystal. These were subtracted using room-temperature data. The intensity contour maps show various patterns at different Bragg-peak positions. Furthermore, the maps at the equivalent Bragg-peak positions on the different scattering plane have different patterns. For example, the 2 2 0 intensity map in the (0 0 1) scattering plane elongates along the direction almost perpendicular to the scattering vector, while that in the (1 −1 0) plane shows small butterfly type. Note that the diffuse scattering intensities in the (0 0 1) scattering plane elongate along the ⟨1 1 0⟩ direction, while those on the (1 −1 0) scattering plane show a slightly steeper slope.

IV. DATA ANALYSIS

From the strong temperature dependence of the intensity, the diffuse scattering was first considered to be magnetic.
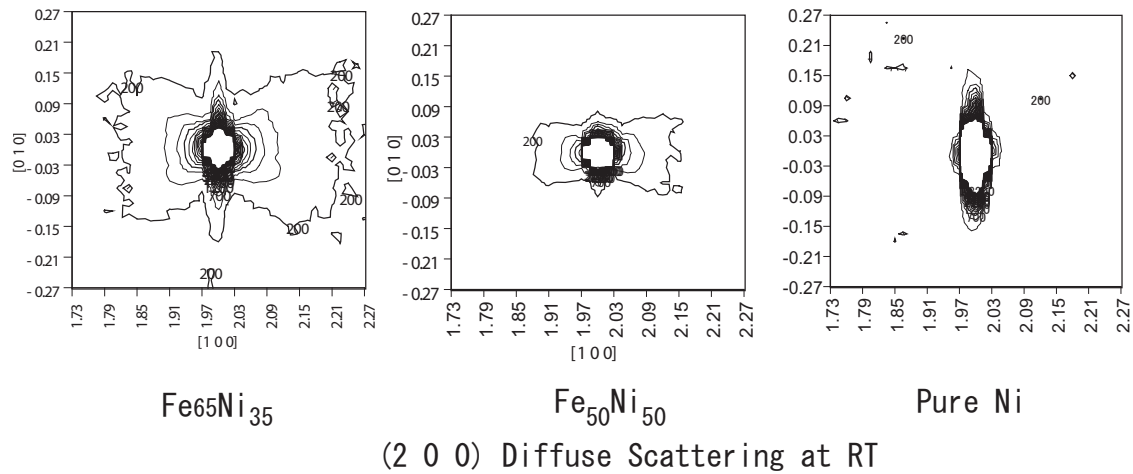
FIG. 2. Diffuse scattering studied around the 2 0 0 Bragg-peak position for several alloys with different Ni concentration. All data were taken at 300 K.

However, this is not the case from the following reasons: (1) Magnetic diffuse scattering for the sample with multiple magnetic domains does not show such a variety of diffuse scattering patterns. (2) The diffuse scattering intensities at various Bragg-peak positions do not follow the rule of the square of the magnetic form factor. (3) We also examined the 2 0 0 diffuse scattering intensity under a magnetic field of 3.5 kOe, which is enough to rearrange the ferromagnetic domains. No appreciable changes were observed in the intensity or the butterfly pattern.

We noticed that the pattern of diffuse scattering intensity observed here has similar symmetry to the distribution of the satellite reflections observed in the low-temperature phase of γ-Fe precipitates in Cu.[14] That is to say, this pattern of dif-

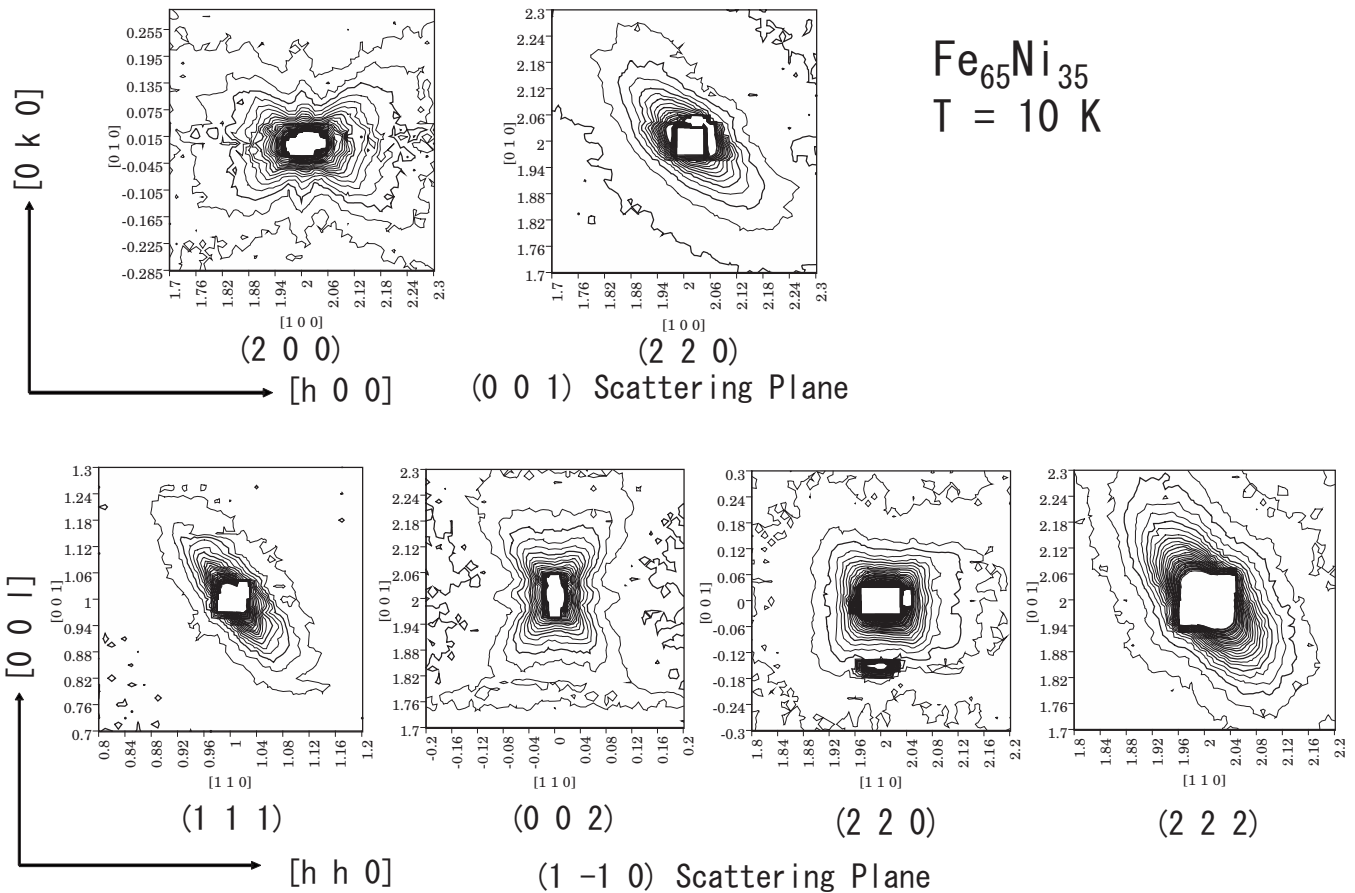
FIG. 3. Elastic diffuse scattering intensity contour maps for $Fe_{65}Ni_{35}$ obtained at various Bragg-peak positions at 10 K. These data were taken at the HB-3 triple-axis spectrometer (HFIR, Oak Ridge) using incident neutrons of 30.5 meV (35 meV for 2 2 2).

fuse scattering comes from clusters which have the same structure as the low-temperature phase of γ-Fe precipitates in Cu. In order to confirm this idea, we tried to reproduce the diffuse scattering patterns at various Bragg-peak positions using simple cluster models.

The lattice structure of the γ-Fe precipitates in Cu in the low-temperature phase is described by periodic shear waves propagating along the $\langle 1\ 1\ 0 \rangle$ direction with the $\langle 1\ -1\ 0 \rangle$ polarization vector in the c plane.[14] If the atomic positions are modulated by a single wave with a wave vector $\mathbf{Q}$ and an amplitude $\mathbf{\Delta}$, $\mathbf{r}_n = na + \mathbf{\Delta}\sin(\mathbf{Q}na)$, then, the scattering intensities are given as

$$I(\mathbf{K}) \propto |f(\mathbf{K})|^2 |\Sigma_n \exp[i\mathbf{K} \cdot (na + \mathbf{\Delta}\sin(\mathbf{Q}na))]|^2$$

$$\propto |f(\mathbf{K})|^2 \sum_{n=0}^{\infty} J_n^2(\mathbf{K} \cdot \mathbf{\Delta}) \delta(\mathbf{K} - \boldsymbol{\tau} \pm n\mathbf{Q}),$$

where f is a scattering amplitude, $\mathbf{K}$ and $\boldsymbol{\tau}$ indicate scattering vector and reciprocal-lattice vector, respectively, and $J_n(t)$ is the nth order spherical Bessel function. The J_0 term gives the normal Bragg peak and J_n gives the nth order satellite. In the present case, $\mathbf{Q}//[1\ 1\ 0]$ and $\mathbf{\Delta} \perp \mathbf{Q}$. Thus, the higher-order satellite peaks appear along the $[1\ 1\ 0]$ direction in reciprocal space if the variable $\mathbf{K} \cdot \mathbf{\Delta}$ has a reasonable value. These satellite peaks were actually observed in the low-temperature phase of the γ-Fe precipitates in Cu up to third order. The wavelength and the amplitude of the shear waves strongly depend on the particle size of the precipitates.[14]

Since the clusters in the FeNi Invar alloys would have various sizes and shapes, the wavelength of the shear wave in the clusters distributes over a wide range. Furthermore, small clusters yield broad coherent peaks. We assumed a Gaussian distribution function of the diffuse scattering intensities extending along the $[1\ 1\ 0]$ direction instead of the satellite reflections. Then, the scattering intensity from the clusters with the shear waves propagating along the $[1\ 1\ 0]$ direction is given as

$$\frac{d\sigma}{d\Omega} \propto |\langle b \rangle|^2 (\mathbf{K} \cdot \mathbf{\Delta})^2 \exp\left[-\frac{\left(\frac{\mathbf{q}_x + \mathbf{q}_y}{\sqrt{2}} \pm \mathbf{Q}\right)^2}{\Gamma_l^2}\right]$$

$$\times \exp\left[-\frac{\left(\frac{\mathbf{q}_y - \mathbf{q}_x}{\sqrt{2}}\right)^2}{\Gamma_t^2}\right] \exp\left[-\frac{\mathbf{q}_z^2}{\Gamma_t^2}\right],$$

where $\langle b \rangle$ is an averaged nuclear scattering amplitude of the alloy, $\mathbf{q}(\mathbf{q}_x,\ \mathbf{q}_y,\ \mathbf{q}_z)$ is a reciprocal-lattice vector measured from the Bragg-peak position, and $\mathbf{\Delta}$ and $\mathbf{Q}$ are the averaged values of the amplitude and the wave vector of the shear wave. $2\Gamma_l$ and $2\Gamma_t$ indicate the FWHM of the Gaussian distribution along the directions parallel to the $[1\ 1\ 0]$ and perpendicular to it, respectively. Since the diffuse peak extends along the $[1\ 1\ 0]$ axis for reasonable values of $\mathbf{K} \cdot \mathbf{\Delta}$, Γ_l should be larger than Γ_t. The clusters with shear waves of all directions equivalent to $[1\ 1\ 0]$ would distribute with equal probability in an Invar alloy sample. Thus, the $\mathbf{q}_x$, $\mathbf{q}_y$, $\mathbf{q}_z$ permutations and $\mathbf{Q}$ and $-\mathbf{Q}$ of Gaussian scattering intensities were considered. Calculated intensity contour maps in

the $(0\ 0\ 1)$ and $(1\ -1\ 0)$ scattering planes using the parameters indicated are given in Fig. 4. The symmetries of the observed diffuse scattering are well reproduced by this simple model. To obtain better agreement with the observed diffuse scattering patterns, the resolution broadening of the spectrometer should be taken into consideration. Since we used vertically focused neutron beams and vertical collimators, the resolution of the direction perpendicular to the scattering plane was rather poor, with the result that the out-of-plane diffuse scattering must be considered. In other words, in the $(1\ -1\ 0)$ scattering plane, there is a shear wave propagating along the $[1\ 1\ 0]$ direction with the polarization vector parallel to the $[1\ -1\ 0]$ direction ($\mathbf{Q}//[1\ 1\ 0]$ and $\mathbf{\Delta}//[1\ -1\ 0]$). This shear wave cannot be observed for the ideal crystal and resolution because the scattering vector $\mathbf{K}$ is always perpendicular to the polarization vector $\mathbf{\Delta}$. All diffuse scattering observed in the $(1\ -1\ 0)$ scattering plane comes from scattering in planes inclined $45°$ to the $(1\ -1\ 0)$ plane. Since this scattering is projected onto the $(1\ -1\ 0)$ scattering plane, diffuse scattering intensities elongate along the $\langle 1\ 1\ -2 \rangle$ direction, which is slightly steeper than $45°$, as observed in Fig. 3. The reason why the butterfly pattern at 0 0 2 in the $(1\ -1\ 0)$ scattering plane is smaller than that at 2 0 0 in the $(0\ 0\ 1)$ plane is also due to the projection into the $(1\ -1\ 0)$ plane for the former. The effect of the resolution correction for the vertical direction is shown in Fig. 5. These situations of the inclusion of out-of-plane components are just the same as the case of γ-Fe precipitates in Cu studied by x-ray diffraction in which the satellite peaks located at out-of-plane were observed as a projection into the scattering plane.

In order to emphasize the similarities with the low-temperature phase of the γ-Fe precipitates in this discussion, we analyzed the experimental data assuming clusters with a lattice deformation of the $\langle 110 \rangle \langle 1\ -1\ 0 \rangle$ shear wave. It is possible to explain the diffuse scattering patterns in a more sophisticated way using Huang diffuse scattering.[15] For instance, a lattice defect such as a nucleus of a low-temperature phase produces a strain field in the surrounding elastic medium. The strain field will be relaxed by the lattice displacement of the medium. This lattice displacement field yields the Huang diffuse scattering. However, the Huang diffuse scattering due to *isotropic point defects* has a pattern with zero intensity for the direction perpendicular to the scattering vector due to the $(\mathbf{K} \cdot \boldsymbol{\delta})^2$ factor of the scattering intensity, where $\mathbf{K}$ is the scattering vector and $\boldsymbol{\delta}$ is an atomic displacement vector. Our experimental data for the 2 2 0 diffuse peak in the $(0\ 0\ 1)$ scattering plane did not show this character, indicating that the Huang diffuse scattering for the isotropic point defect is not applicable to the present case. Thus, we tried to calculate the Huang diffuse scattering for *anisotropic defects*[15] using the reported values of the elastic constants $(C_{11} = 13.5,\ C_{12} = 10.5,\ \text{and}\ C_{44} = 10.0\ \text{N}/\text{m}^2)$ for $Fe_{65}Ni_{35}$ alloy.[3] Reasonable agreement with the observed intensity maps was obtained for the double-force matrix with a tetragonal symmetry and with $c/a > 1$. Detailed analysis of Huang diffuse scattering will be published elsewhere [the paper was submitted to IUCr 2008 (Osaka)]. From the Huang diffuse scattering data analysis, however, it is hard to imagine what kind of lattice deformation was induced in the
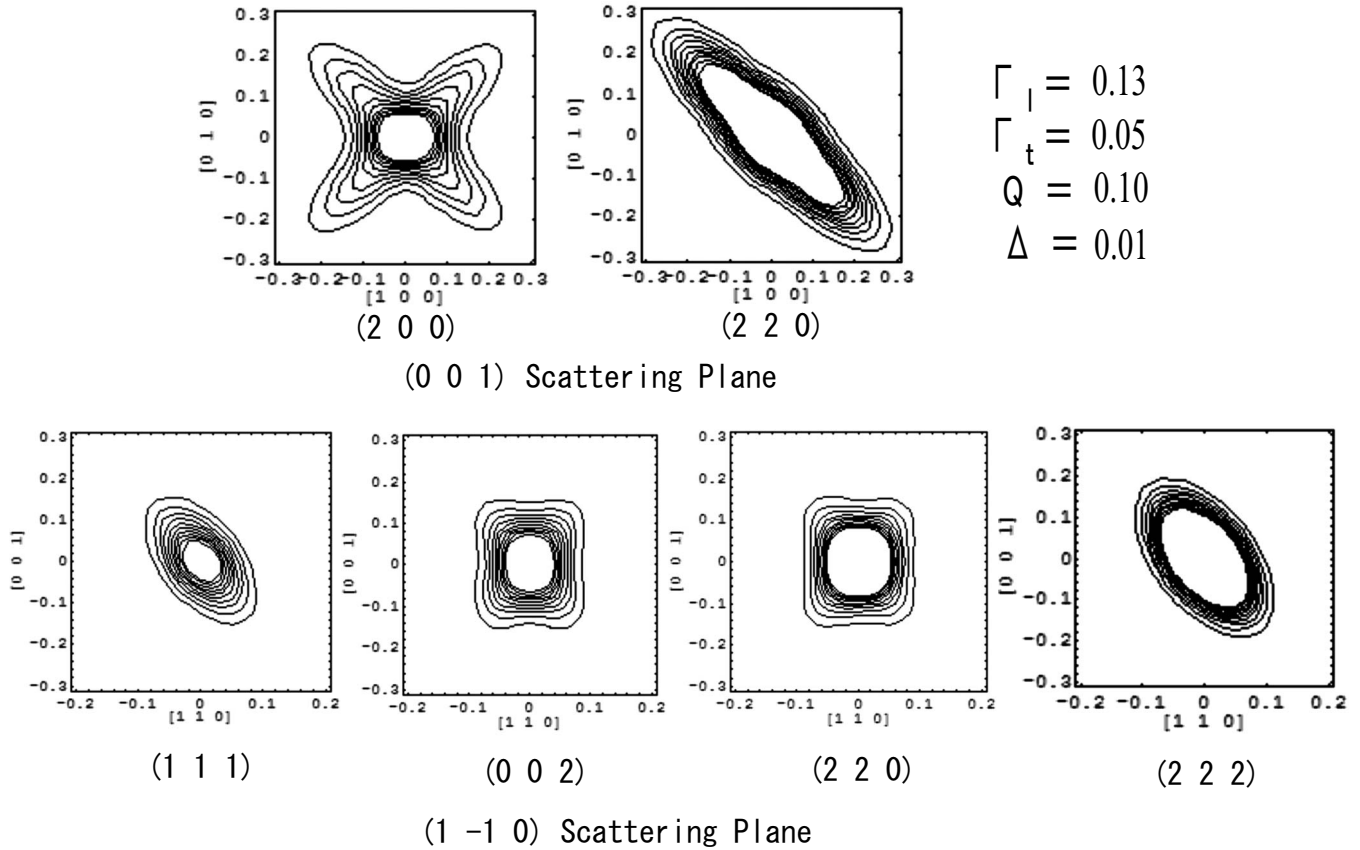
FIG. 4. Calculated intensity contour maps around several Bragg-peak positions on the (0 0 1) and (1 −1 0) scattering planes using the equations described in the text. For the parameters, see text.

surrounding elastic medium. Thus, we tried to calculate the Huang diffuse scattering intensity maps in various scattering planes in three-dimensional reciprocal space and compared them with those for the simple Gaussian model described above. These diffuse scattering intensity maps in various scattering planes show almost the same patterns as those for the simple Gaussian model. That is to say, the calculated Huang diffuse scattering intensity extends along the 12 equivalent $\langle 1\ 1\ 0 \rangle$ directions and the patterns are determined by the intensity selection rule of the $(\mathbf{K} \cdot \mathbf{\Delta})^2$ factor. Thus, no matter which analysis we use, what happens in the

FeNi Invar alloys is the same. There are clusters with the lattice deformation with a shear wave propagating along the $\langle 1\ 1\ 0 \rangle$ direction and with the $\langle 1\ -1\ 0 \rangle$ polarization vector.

V. SUMMARY AND DISCUSSION

ASRO of the $Fe_{65}Ni_{35}$ sample, for which most of the present data were taken, was checked around the (1 0 0) and (1 1 0) Bragg-peak positions. The data are given in Fig. 6. These data were taken under the same condition as the diffuse scattering measurements at the T1-1 spectrometer. No
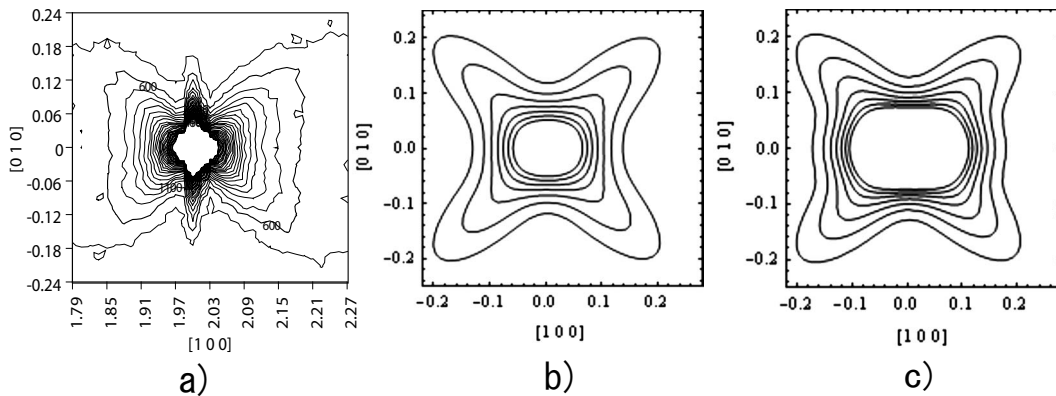

FIG. 5. Correction due to the vertical resolution. (a) Experimental data obtained around the 2 0 0 reciprocal-lattice point. (b) Calculated intensity without resolution correction. (c) Calculated intensity including the vertical out-of-plane components.
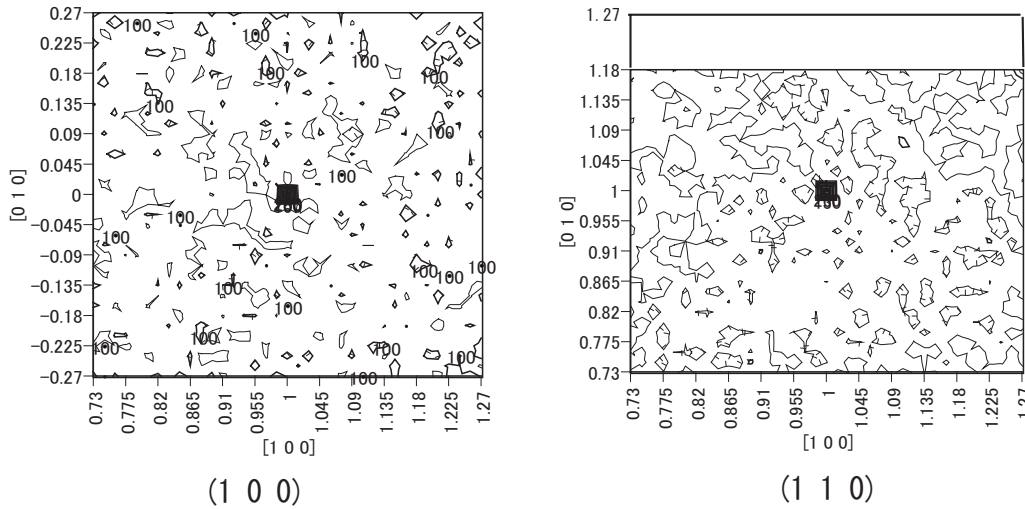
FIG. 6. Intensity maps obtained around the 1 0 0 and 1 1 0 Bragg-peak positions for checking the atomic short-range order. Sharp peaks at the 1 0 0 and 1 1 0 reciprocal lattice points are the $\lambda/2(200)$ and $\lambda/2(220)$ Bragg peaks, respectively, arising from imperfect filtering of higher-order component.

trace of the ASRO peak was observed. Since the nuclear scattering amplitudes of Fe and Ni are rather close (b_{Fe} =9.51 fm and b_{Ni}=10.3 fm), the neutron-scattering method is not sensitive to the ASRO of FeNi system for nuclear scattering, but magnetic diffuse scattering should be observed if the ASRO exists because of the large difference in the sizes of the magnetic moments for Fe and Ni atoms. Thus, we can safely say that the present sample is almost a random alloy.

From the parameters used in the calculation of the simplified Gaussian model to reproduce the diffuse peak patterns, we can roughly estimate the averaged values of the shear waves in the clusters. The wave vector **Q** [0.08–0.13 in $(2\pi/a)$ unit] would be a measure of the diameter of clusters. We can estimate the average size of the clusters to be 2–5 nm. The amplitude of the shear wave $\mathbf{\Delta}$, which is related to the diffuse scattering intensity, cannot be determined from the present experimental data because we do not know the density of the clusters. However, if $\mathbf{\Delta}$ is very small, we would not observe diffuse scattering. Since the diffuse scattering intensities were comparable to the low-energy phonon intensities, $\mathbf{\Delta}$ could be estimated to be the order of $0.01a$, where a is the lattice parameter.

As shown in Fig. 1, change in the diffuse scattering intensity below room temperature is rather remarkable. This is another reason why the diffuse scattering is not magnetic in origin. The diffuse scattering intensity depends on two factors, the density of clusters and the amplitude of lattice deformation. Both factors may change with temperature.

As pointed out in Sec. I, the cause of the Invar effect has long been considered to be from the magnetism of fcc Fe. Although recent neutron-scattering measurements show rather negative results for the well-known Weiss's 2γ-state model,[11,12] there is no doubt that the Invar effect is strongly related to the magnetism of the alloys as described in various experimental reports on the Invar effect such as the large spontaneous magnetovolume effect. Apart from the Weiss's 2γ-state model, Shiga[17] derived the interrelation between the

volume and the localized magnetic moment using the renormalized spin-fluctuation theory developed by Moriya.[18] The present experiments show that the temperature variation and the concentration dependence of the Invar anomalies observed in FeNi alloys almost coincide with those of the diffuse scattering intensities observed here. Furthermore, diffuse scattering with the same patterns as the FeNi Invar alloys was also observed for another typical Invar alloy, ordered and disordered Fe_3Pt.[16] Thus, the appearance of the clusters with the shear wave seems to be strongly correlated with the Invar effect. When we consider the magnetism of the deformed clusters, we are reminded of the γ-Fe precipitates in Cu. Mössbauer spectroscopy data reported by Ezawa *et al.*[19] show that γ-Fe precipitates in small sizes, which are retained in the cubic lattice and have a spiral spin structure,[20] have a rather small hyperfine field ($\sim$1.6 T) and low Néel temperature ($\sim$40 K). However, the γ-Fe precipitates grown up to larger sizes, which undergo a structural phase transition to the state with the lattice deformation described by the $\langle 110 \rangle \langle 1\ -1\ 0 \rangle$ shear wave, show a different magnetic structure with roughly twice the hyperfine field and twice the Néel temperature ($\sim$3 T and $\sim$70 K) as those in the cubic state. The results suggest that the magnetic moments in the deformed lattice of the γ-Fe precipitates are larger than those in the ideal cubic lattice. Similarly, in FeNi Invar alloys, the Fe atoms in the clusters with the lattice deformation of the $\langle 110 \rangle \langle 1\ -1\ 0 \rangle$ shear wave are also likely to have different magnetic moments from those in the surrounding cubic structure. Hesse[21] reported that the hyperfine field H(n) in $Fe_{65}Ni_{35}$ Invar alloy as a function of nearest-neighbor Fe number n abruptly decreases at $n=10$ due to the antiparallel coupling of the spins. However, no direct evidence from neutron-scattering data showing antiparallel spin coupling has been reported. The abrupt change in H(n) might be due to the lattice deformation in the clusters. This phenomenon could be observed by the careful examination of the neutron diffuse scattering intensities, but the magnetic contribution would be rather weak and very careful measurements are

required. These experiments will be done at a future date.

Now, we consider the possible causes of the deformed clusters with the $\langle 110 \rangle$ $\langle 1\ -1\ 0 \rangle$ shear wave. One cause is a nucleus of Fe-rich cluster with the high spin and large volume. The other is the precursor embryos of the fcc-bcc martensitic transformation in FeNi alloys.

A. High-volume Fe rich clusters

Recent x-ray diffuse scattering experiments for FeNi Invar alloys using synchrotron radiation reported that the nearest-neighbor atomic distance of Fe-Fe pair is larger than those of Fe-Ni and Ni-Ni and the difference increases with lowering temperature.[22,23] A weak tendency for Fe atoms to form {1 0 0} platelets extending about ∼0.9 nm in diameter is also reported.[23] The results indicate that the Fe-rich platelets have expanding volumes at low temperature. Then, the Fe-rich platelets with expanded volume could become the nucleus of the Huang diffuse scattering. Since an atomic diffusion is considered to be suppressed below room temperature, large increases in the diffuse scattering intensities below room temperature would be explained by the low-spin–high-spin (small-volume–large-volume) transition of Fe moments with decreasing temperature.

B. Precursor embryos of the fcc-bcc martensitic transformation

In the data analysis, we showed that the distribution of diffuse scattering intensities at various Bragg-peak positions are well explained by clusters with the lattice deformation of shear wave propagating along $\langle 110 \rangle$ and polarized along the $\langle 1\ -1\ 0 \rangle$ direction. This lattice structure coincides with that observed in the low-temperature phase of γ-Fe precipitates in Cu reported by one of the present authors.[14] In the latter, γ-Fe precipitates are constrained to be the fcc structure due to the coherent binding forces with Cu matrix but have an inherent driving force toward the bcc structure. With decreasing temperature, the precipitates start undergoing the martensitic transformation from fcc to bcc structure. However, lattice expansion and external shape change are strictly suppressed by the Cu matrix, resulting in the *periodic* shear wave propagating along the $\langle 110 \rangle$ direction with $\langle 1\ -1\ 0 \rangle$ polarization vector. This situation was well reproduced by the molecular-dynamics simulations.[24] The possibility of a transitional state of fcc-bcc martensitic transformation in γ-Fe precipitates in Cu was discussed in a previous paper.[25]

These features of γ-Fe precipitates seem to be common to the clusters with the lattice deformation in FeNi Invar alloys and suggest that these clusters could be the embryos of the fcc-bcc martensitic transformation in FeNi alloys. Since the FeNi alloys showing the Invar effect are very close to the phase boundary of the fcc-bcc martensitic transformation, temperature and concentration dependences of the diffuse scattering intensities are well understood as a premartensitic phenomenon.

The lattice softening with decreasing temperature for the shear phonon mode along the [1 1 0] direction (T_1 mode) and for the elastic modulus C' [$=(C_{11}-C_{12})/2$] in FeNi Invar alloys were reported more than two decades ago.[26,27] Since the lattice softening started around the Curie temperature (T_c), the authors discussed the causes of lattice softening in relation to the magnetism of the alloys rather than the fcc-bcc martensitic transformation. The appearance of pre-martensitic embryos also starts around T_c because the ferromagnetic ordering reduces relative lattice energy of bcc structure to that of fcc as many first-principles calculations show.

A superior point of the precursor embryo model is that we do not have to use the 2γ-state model which has not been proved definitively by experiments. Especially, diffuse scattering with the same patterns as FeNi Invar alloys is also observed for another typical Invar alloys, ordered and disordered Fe_3Pt, for which the 2γ-state model is not accepted.[3] Both FeNi and Fe_3Pt alloys, which show the Invar effect, are located close to the phase boundary of fcc-bcc martensitic transformation, and elastic diffuse scattering with the same patterns is the characteristic common to both systems, strongly supports the clusters with the lattice deformation of $\langle 1\ 1\ 0 \rangle$ $\langle 1\ -1\ 0 \rangle$ shear wave as the precursor embryos of the fcc-bcc martensitic transformation in these alloys.

The most important problem we have to discuss would be how the appearance of clusters with lattice deformation is related to the Invar effect. Since the shear deformation of the lattice along the [1 1 0] direction does not include the volume expansion, the appearance of clusters with lattice deformation would not be the direct cause of the lattice expansion with decreasing temperature. The special electronic states, which lead the fcc lattice to instability, would rather play an important role to the Invar effect. As one of such causes, we can suspect the strong interatomic Coulomb correlations of d electrons. As the number of carriers (holes for the present case) increases, the collision probability during electron hopping increases. Since there are many (12) nearest-neighbor atoms in the fcc lattice, the lattice expands to reduce the probability of electron collisions. By further increasing number of carriers, a bcc structure would become more stable because a bcc structure has only eight nearest-neighbor atoms. Thus, the Invar alloys are considered to be a transitional state from fcc to bcc structures and the appearance of clusters with lattice deformation would be one of the Invar phenomena. Unfortunately, it is very hard to verify the importance of interatomic Coulomb correlations experimentally.

VI. CONCLUSION

We found elastic diffuse scattering of neutrons around various Bragg-peak positions of FeNi Invar alloys. The diffuse scattering intensities elongate along the $\langle 1\ 1\ 0 \rangle$ directions on the (0 0 1) scattering plane and the $\langle 1\ 1\ -2 \rangle$ directions on the (1 −1 0) scattering plane. The diffuse scattering intensity depends on temperature and Ni concentration of the alloys and increases with decreasing temperature and decreases with increasing Ni concentration. The patterns of the diffuse peak intensity contour maps at various Bragg-peak positions are well explained by clusters with a lattice deformation wave propagating along the $\langle 1\ 1\ 0 \rangle$ direction with a $\langle 1\ -1\ 0 \rangle$ polarization vector. As origin of diffuse scattering, two possible explanations are given. The

one is the Huang diffuse scattering due to the nucleus of Fe rich clusters in the high-spin state and large volume. The other is the appearance of premartensitic embryos with a lattice deformation toward the fcc-bcc martensitic transformation of FeNi alloys.

Since the temperature and Fe concentration of the alloys, for which the Invar effect is observable, coincide with those for which diffuse scattering is observed, the appearance of the clusters with the lattice deformation seems to be strongly related to the causes of the Invar effect. However, this kind of local lattice deformation has not been taken into consideration in the discussion of Invar properties. The local lattice deformation in the clusters itself may not be a direct origin of the Invar effect. However, the special electronic state which leads the fcc lattice to instability would be rather strongly correlated with the Invar effect. The present experimental data imply that Invar alloys are inhomogeneous systems containing clusters with a $\langle 1\ 1\ 0 \rangle\ \langle 1\ -1\ 0 \rangle$ shear wave lattice deformation.

ACKNOWLEDGMENTS

[1] C. E. Guillaume, C. R. Acad. Sci. **125**, 235 (1897).

[2] R. J. Weiss, Proc. R. Soc. Edinb [Biol] **82**, 281 (1963).

[3] E. F. Wasserman, *Ferromagnetic Materials*, edited by K. H. J. Buschow and E. P. Wahlfarth (North-Holland, Amsterdam, 1990), Vol. 5, pp. 237–322.

[4] V. L. Moruzzi, Phys. Rev. B **41**, 6939 (1990).

[5] P. Entel, E. Hoffmann, P. Mohn, K. Schwarz, and V. L. Moruzzi, Phys. Rev. B **47**, 8706 (1993).

[6] H. Akai and P. H. Dederichs, Phys. Rev. B **47**, 8739 (1993).

[7] I. A. Abrikosov, O. Eriksson, P. Soderlind, H. L. Skriver, and B. Johansson, Phys. Rev. B **51**, 1058 (1995).

[8] M. Uhl and J. Kubler, J. Phys.: Condens. Matter **9**, 7885 (1997).

[9] Y. Wang, G. M. Stocks, D. M. C. Nicholson, W. A. Shelton, V. P. Antropov, and B. N. Harmon, J. Appl. Phys. **81**, 3873 (1997).

[10] M. van Schilfgaarde, I. A. Abrikosov, and B. Johansson, Nature (London) **400**, 46 (1999).

[11] N. Cowlam and A. R. Wildes, J. Phys.: Condens. Matter **15**, 521 (2003).

[12] P. J. Brown, K.-U. Neumann, and K. R. A. Ziebeck, J. Phys.: Condens. Matter **13**, 1563 (2001).

[13] The Invar alloys" may be defined for the very narrow Ni concentration range with almost zero lattice expansion coefficient. Here, we use it for rather wide Ni concentration range for which anomalous thermal expansion is observed.

[14] Y. Tsunoda and N. Kunitomi, J. Phys. F: Met. Phys. **18**, 1405 (1988).

[15] P. H. Dederichs, J. Phys. F: Met. Phys. **3**, 471 (1973).

[16] Preliminary experiments for both ordered and disordered $Fe_{72}Pt_{28}$ alloys showed temperature-dependent elastic diffuse scattering with the same butterfly pattern to the $Fe_{65}Ni_{35}$ alloy. Full data will be published elsewhere.

[17] M. Shiga, *Material Science and Technology*, edited by R. W. Cahn, P. Haasen, and E. J. Kramer (VCH, Verlagsgesellschaft, Weinheim, 1993), Vol. 3B, pp. 159–210.

[18] T. Moriya and A. Kawabata, J. Phys. Soc. Jpn. **34**, 639 (1973); **35**, 669 (1973).

[19] T. Ezawa, W. A. A. Macedo, U. Glos, W. Keune, K. Schletz, and U. Kirschbaum, Physica B (Amsterdam) **161**, 281 (1989).

[20] Y. Tsunoda, J. Phys.: Condens. Matter **1**, 10427 (1989).

[21] J. Hesse, Hyperfine Interact. **47**, 357 (1989).

[22] X. Jiang, G. E. Ice, C. J. Sparks, L. Robertson, and P. Zschack, Phys. Rev. B **54**, 3211 (1996).

[23] J. L. Robertson, G. E. Ice, C. J. Sparks, X. Jiang, P. Zschack, F. Bley, S. Lefebvre, and M. Bessiere, Phys. Rev. Lett. **82**, 2911 (1999).

[24] A. Silberstein and P. C. Clapp, Phys. Rev. B **38**, 9555 (1988).

[25] Y. Tsunoda, J. Phys. Soc. Jpn. **58**, 1648 (1989).

[26] Y. Endoh, Y. Noda, and Y. Ishikawa, Solid State Commun. **23**, 951 (1977).

[27] G. Hausch and H. Warlimont, Acta Metall. **21**, 401 (1973).